NASA TECHNICAL NOTE

NASA TN D-6957

NASA TN D-6957

EXPERIMENTAL DYNAMIC RESPONSE OF A TWO-DIMENSIONAL, MACH 2.7, MIXED-COMPRESSION INLET

by Robert J. Baumbick, George H. Neiner, and Gary L. Cole

Lewis Research Center
Cleveland, Ohio 44135

NATIONAL AERONAUTICS AND SPACE ADMINISTRATION • WASHINGTON, D. C. • SEPTEMBER 1972

1. Report No.	2. Government Accession No.	3. Recipient's Catalog No.
NASA TN D-6957		

4. Title and Subtitle	5. Report Date
EXPERIMENTAL DYNAMIC RESPONSE OF A TWO-DIMENSIONAL, MACH 2.7, MIXED-COMPRESSION INLET	September 1972
	6. Performing Organization Code

7. Author(s)	8. Performing Organization Report No.
Robert J. Baumbick, George H. Neiner, and Gary L. Cole	E-7002
	10. Work Unit No. 764-74

9. Performing Organization Name and Address	11. Contract or Grant No.
Lewis Research Center National Aeronautics and Space Administration Cleveland, Ohio 44135	

12. Sponsoring Agency Name and Address	13. Type of Report and Period Covered
National Aeronautics and Space Administration Washington, D.C. 25046	Technical Note
	14. Sponsoring Agency Code

15. Supplementary Notes

16. Abstract

A test program was conducted on a two-dimensional supersonic inlet. Internal disturbances in diffuser exit mass flow were produced by oscillating overboard bypass doors. Open-loop dynamic responses of shock position, throat exit and diffuser exit static pressures are presented. The steady-state and dynamic coupling between ducts were also obtained. The experimental results from the two-dimensional inlet are compared to results from a similar size axisymmetric inlet and also to a transfer function synthesis program.

17. Key Words (Suggested by Author(s))	18. Distribution Statement
Supersonic inlets Air intakes Supersonic inlet dynamics Two-dimensional inlets	Unclassified - unlimited

19. Security Classif. (of this report)	20. Security Classif. (of this page)	21. No. of Pages	22. Price*
Unclassified	Unclassified	30	$3.00

* For sale by the National Technical Information Service, Springfield, Virginia 22151

EXPERIMENTAL DYNAMIC RESPONSE OF A TWO-DIMENSIONAL MACH 2.7, MIXED-COMPRESSION INLET

by Robert J. Baumbick, George H. Neiner, and Gary L. Cole

Lewis Research Center

SUMMARY

A test program was conducted on a two-dimensional supersonic inlet. Internal disturbances in diffuser exit mass flow were produced by oscillating overboard bypass doors. Open-loop dynamic responses of shock position, throat exit and diffuser exit static pressures are presented. The steady-state and dynamic coupling between ducts were also obtained. The inlet was run with and without a splitter plate. The splitter plate is an extension of the ramp and extends to the choked orifice plate. Response for the inlet at various angles-of-attack at an off-design Mach number and with different bleed configurations are presented and compared to results for the design operating conditions.

The experimental results from the two-dimensional inlet are compared to results from a similar size axisymmetric inlet and also to a transfer function synthesis program.

INTRODUCTION

The increased use of supersonic aircraft requires new, sophisticated inlet systems and inlet controls to insure that the engine is supplied with the proper airflow and pressure distribution. Problems, unique to the supersonic flow regime, demand reliable methods for operation and control of these inlets. The inlet's function is to convert the kinetic energy of the moving air into potential energy (static pressure rise). In addition, the inlet must present the compressor with a uniform pressure distribution.

Inlet efficiency is a strong function of terminal shock position; therefore, holding the shock at a given position in the inlet is of paramount importance. To develop a good shock position sensor and shock position control, the inlet's dynamic characteristics must be defined; then, suitable controls can be developed. The inlet may be subjected

to internal and external disturbances which tend to move the terminal shock from its design point. The final control must, therefore, be capable of minimizing the effects of these disturbances on terminal shock position.

Experimental tests of these shock dynamics were conducted on a two-dimensional inlet in the Lewis 10- by 10-Foot Supersonic Wind Tunnel. This inlet has a wedge-shaped, collapsible centerbody. Seventy percent of the supersonic area concentration occurs externally at the inlet design Mach number of 2.7. The inlet is referred to as a 70-30 two-dimensional inlet. The inlet is separated into two ducts. Each duct is equipped with a pair of servodriven overboard bypass doors and performance bleed ports which are located on the centerbody and cowl.

Previous work with inlets is reported in references 1 to 4. The response of a Mach 2.5 axisymmetric inlet, with different terminations, is reported in reference 1. The inlet was subjected to both internal and external disturbances. Reference 2 presents results for both internal and external disturbances introduced to an inlet operating at Mach 3. In these tests, measurement of terminal shock position, throat exit static and diffuser exit static pressures were made. A mathematical analysis of supersonic inlet dynamics is presented in reference 5.

In the current series of tests open-loop dynamic tests were conducted to define the inlet's dynamic characteristics. To obtain these results, the inlet was subjected to internal disturbances by oscillating an overboard bypass door in each duct. This produced changes in diffuser exit mass flow. The response of throat exit and diffuser exit static pressure and terminal shock position to this disturbance was measured. Results are presented for both design and off-design conditions.

Tests were conducted to determine the coupling between ducts when the disturbance was introduced in one duct. All the results presented herein were obtained by oscillating one bypass door. Coupling effects between the two ducts are shown.

A transfer function synthesis program was used to represent the experimental data with a simplified transfer function. The results obtained from this program provided a relatively simple transfer function which adequately described the dynamic characteristics of the inlet over the frequency range considered. Comparisons between the analytical program results and experimental data are presented.

APPARATUS AND PROCEDURE

Model

Two views of the inlet are shown in figures 1 and 2. The inlet is a two-dimensional, mixed-compression inlet with a wedge-type, collapsible centerbody. The inlet is designed for operation at Mach 2.7 with 70 percent of the supersonic area contraction

occurring externally at the design Mach number. The corresponding free stream conditions were total pressure of 9.55 N/cm^2, total temperature of 320 K, specific heat ratio of 1.4, and test section Reynolds number of 7.75×10^6 per meter. The inlet is separated into two ducts and has a removable splitter plate attached to the aft end of the centerbody and extended to an orifice located approximately at the compressor face plane. The splitter plate is shown in figures 2 and 3. The orifice operates choked. A comparison of inlets terminated in an orifice, a long cold pipe, and a turbojet engine is presented in reference 1. It was shown that the choked orifice termination more closely represents a turbojet termination as far as the inlet responses are concerned.

Each duct is equipped with bleed ports and vortex generators located on the centerbody, cowl, and sidewalls. In addition, each duct is equipped with a pair of overboard bypass doors, located on the cowl, downstream of the geometric throat. Figure 1 illustrates the location of the bypass doors, collapsible ramp, and throat bleed pipes. The bleed flow can be varied by means of retractable plugs that terminate the throat bleed pipes. Figure 2 is a cutaway view, showing the bleed ports and the internal configuration of the collapsible ramp.

The inlet is 180.34 centimeters long and has a capture area of 2220 square centimeters.

Test Configurations

The design operating point for this inlet is at a free stream Mach number of 2.7. The design operating configuration was at zero angle-of-attack with the splitter plate extension in position and with the minimum bleed flow, which provided high levels of performance. Other cases run were with splitter plate extension removed, a $\pm 2^{\circ}$ angle-of-attack, larger geometric throat area (1.04 times design area), and a Mach number of 2.3. A case was also run with maximum bleed flow.

Disturbance Device

Each duct is equipped with a pair of overboard bypass doors. Each door assembly consists of two slotted plates. On plate is fixed on the cowl. The second plate moves relative to this fixed plate. Each door has four slots. The dimension of each slot is 19.05 by 2.54 centimeters. The door motion for these tests was 0.42 centimeter (maximum) peak-to-peak, providing a peak-to-peak area change of 32 square centimeters. Each door is driven by a high-response, two-stage electrohydraulic servovalve and hydraulic actuator combination. Detailed information on the servosystem is presented in reference 6. The dynamic response of the bypass door assembly, shown in figure 4, is flat to 100 hertz. This response, typical for these tests, is for a peak-to-

peak door movement of 0.42 centimeter (16 percent of full travel). All four doors were tuned to yield approximately the same response shown in figure 4.

One bypass door was sued to produce an internal disturbance in the inlet. The other three doors remained at their design operating point. Since the bypass door flow was choked, the real effect of oscillating the door was to produce changes in the diffuser exit mass flow which corresponded to the changes in door flow area.

Instrumentation

Pressure measurements were made with strain gage transducers connected to the cowl with short tubes (6.35 cm (maximum)). The tubes were provided with orifices which extended the frequency response of the measuring system. The transducer response had less than 1 decibel attenuation and negligible phase shift over the frequency range (1 to 150 Hz) considered in these tests.

The location of the pressure transducers in each duct is shown in figure 3. Eight transducers ($P_{u,a}$ to $P_{u,h}$ and $P_{\ell,a}$ to $P_{\ell,h}$) are located on the cowl, 8.64 centimeters off the inlet's centerline. These transducers, located in the inlet's throat region were used as the shock position sensor (ESP_u for upper duct and ESP_ℓ for lower duct). The throat exit static pressures ($P_{u,57}$, $P_{\ell,57}$) and the diffuser exit static pressures ($P_{u,87}$, $P_{\ell,87}$) were also measured. The numbers 57 and 87 indicate the distance from the cowl lip in centimeters.

Shock Sensor

Terminal shock was determined by an electronic shock sensor. Inputs to the sensor were the outputs of the eight throat static pressures. These taps were evenly spaced in both upper and lower ducts. The spacing between these taps was 1.27 centimeters. Each throat static pressure output was compared to a reference pressure. As the terminal shock moved upstream, a constant voltage level was turned on for each tap having a higher output than the reference. The terminal shock was considered to be between the tap that had a higher output than the reference and the adjacent pressure tap. The constant voltage levels switched in were summed by an analog amplifier. This resulted in a shock sensor output that was a stepwise-continuous function proportional to shock position. Sensor resolution is limited to the spacing of the pressure taps.

The reference pressure used for switching was 0.528 times the total pressure measured at the inlet's geometric throat. The responses shown for the shock position

represent the output of this shock sensor to a disturbance in diffuser exit mass flow caused by a change in bypass door area. The following sketch illustrates the output of the shock sensor:

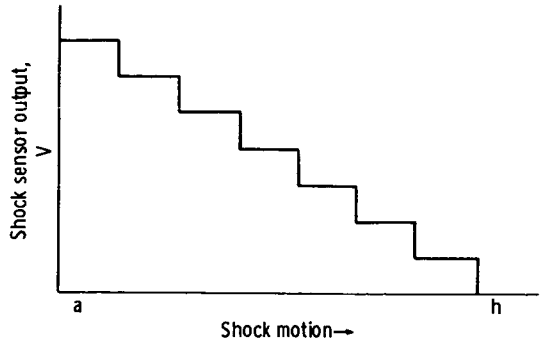

Data Reduction

The method used consisted of initial on-line analysis using a commercial frequency response analyzer. The analyzer output was then used as the input to a digital program which put the data into the desired form. Results are presented as amplitude ratios and phase differences. The responses represent the change in shock position and pressures to changes in bypass door area. The data are normalized by dividing the amplitude ratio of each signal by their value at 1 hertz.

RESULTS AND DISCUSSION

Large noise content was present in the variables measured. A cause of noise could be due to an inherent instability in shock position. Figure 5 is a strip chart recording of upper duct pressures as the terminal shock moves from a position upstream of transducer $P_{u,a}$ toward the aft end of the inlet. Shock motion was produced by slowly ramping the overboard bypass doors from a closed to an open position. Shown in figure 5 are pressures $P_{u,a}$, $P_{u,b}$, $P_{u,c}$, $P_{u,d}$, $P_{u,e}$, $P_{u,f}$, and $P_{u,h}$ which make up the shock sensor. Pressure $P_{u,g}$ was not recorded. Also shown in this figure are the throat exit static pressure $P_{u,57}$ and the diffuser exit static pressure $P_{u,87}$. As the bypass doors open, the shock moves across the pressure taps. An instability occurs in the transition from subsonic to supersonic conditions. With the doors fully open, the terminal shock is in the region between $P_{u,h}$ and $P_{u,57}$. It is apparent from the figure that the shock instability is reflected as far upstream as pressure $P_{u,c}$. The

operating point has the terminal shock positioned between $P_{u,c}$ and $P_{u,d}$. The shock instability is also reflected in the throat exit static pressure $P_{u,87}$.

A condition that may be responsible for this shock instability is that the transition is too abrupt from the square to circular cross section of the diffuser.

Open-Loop Results

Figures 6 to 10 show the response of shock position ESP_u, $P_{u,h}$, throat exit static pressure $P_{u,57}$, and diffuser exit static pressure $P_{u,87}$ to perturbations in diffuser exit mass flow. Diffuser exit mass flow was changed by oscillating the overboard bypass door. The range of disturbance frequencies was 1 to 150 hertz.

A splitter plate was installed to separate the upper and lower duct. It extended from the aft end of the ramp to the compressor face plane. Addition of the splitter plate significantly reduced the coupling between ducts, but complete isolation was not achieved. The coupling between ducts is not significantly affected by the amount of bleed flow. The coupling data discussed hereinafter was obtained with minimum bleed flow. A disturbance introduced into the upper duct by varying the bypass door area produced changes in lower duct pressures. The steady-state gain between the pressure $P_{u,h}$ (last tap of the upper duct shock sensor) and bypass door area change was 0.050 $N/cm^2/cm^2$. The gain for $P_{\ell,h}$ (last tap of lower duct shock sensor) to upper duct bypass door area change was 0.008 $N/cm^2/cm^2$. Similar gains for the throat exit static pressures were 0.027 $N/cm^2/cm^2$ and 0.003 $N/cm^2/cm^2$. These gains were obtained for a peak-to-peak area change of 32 square centimeters. Figure 11 illustrates the dynamic response of lower duct signals for upper duct disturbance with and without the splitter plate extension. There is approximately 12 to 20 percent steady-state coupling with splitter plate against 39 to 57 percent steady-state coupling with splitter plate out. Data for the splitter plate in were only obtained out to 25 hertz.

Dynamic response of upper duct signals to bypass door disturbance in the upper duct are shown in figure 6. These responses are for the design operating point with the inlet at zero angle-of-attack, splitter plate extension in, minimum bleed flow, and free stream Mach number of 2.7. The response of shock position ESP_u, pressure $P_{u,h}$, and throat exit static pressure $P_{u,57}$ all show a slight attenuation beginning below 10 hertz. The response of $P_{u,87}$ is flat to approximately 15 hertz. Beyond this the response resembles a first order lag in the 20 to 60 hertz range. A resonance is detected at approximately 100 hertz. In the 100 hertz region the response of ESP_u, $P_{u,h}$, and $P_{u,57}$ indicate higher damping.

Tests were conducted to check the similarity of upper and lower ducts. The results showed that both ducts have similar dynamic characteristics.

Tests were also conducted for effects, upon dynamic response, of maximum bleed flow. The results showed that the response of the selected variables were relatively insensitive to bleed conditions.

Other configurations were run, including a larger geometric throat area (1.04 times the design area), $\pm 2^{\circ}$ angle-of-attack, and operation at a free stream Mach number of 2.3. These responses are shown in figures 7 to 10. These figures include, for comparison, the results for the design operating case. The design conditions were run at a free stream Mach number of 2.7, zero angle-of-attack, and a small amount of bleed flow. The most significant difference in response occurs for Mach 2.3 operation (refer to fig. 10).

The splitter plate extension was removed and frequency responses were taken. A comparison of responses with and without splitter plate is shown in figure 12. This figure illustrates the difference in response for ESP_u, $P_{u,57}$, and $P_{u,58}$ for a disturbance produced in the upper duct by varying the bypass door area.

Figure 13 compares the response of shock position, throat exit static, and diffuser exit static pressures of the 70-30 two-dimensional inlet with similar signals from a 40-60 axisymmetric inlet. The responses for the 70-30 inlet are for half of the total inlet (inlet separated into two ducts by the splitter plate), the design case as shown in figure 7. The transducer locations for the 40-60 inlet are illustrated in reference 4.

Open-Loop Transfer Function

Considerable time savings and subsequent cost reductions can be realized if the model's open-loop dynamics can be accurately described by a transfer function. Selection of suitable controls and control optimization studies could be done on the computer if the open-loop dynamics can be expressed analytically. The results could then be used in the test cell, eliminating the time normally used in testing to achieve these objectives. This approach could result in shorter overall testing programs.

A program for synthesizing transfer functions was used for the data from this inlet program. The transfer functions obtained, together with the experimental dynamic characteristics are shown in figure 14. The results show a normalized response for throat exit static and diffuser exit static pressure to bypass door area change. These responses are for upper duct signals.

SUMMARY OF RESULTS

Dynamic responses of a two-dimensional inlet are presented. The response of three variables: shock position, throat exit, and diffuser exit static pressures to a

change in diffuser exit mass flow are presented. The inlet was disturbed by oscillating an overboard bypass door. The frequency range covered in these tests was 1 to 150 hertz.

The dynamic responses of the three variables show attenuation starting at about 10 hertz with a damped resonance at approximately 100 hertz. The response of the throat and diffuser exit static pressures show less attenuation at the higher frequencies and less damping of resonance. The two ducts of the inlet are similar in dynamic response. Results show that the inlet's dynamic characteristics are relatively insensitive to the amount of bleed flow. A different response, with less attenuation in the midfrequency range of 10 to 60 hertz, was obtained by running the inlet at free stream Mach number 2.3.

The addition of the splitter plate changes the dynamic response of the inlet. The splitter plate is an extension of the ramp to the choked orifice plate. A comparison of responses with and without the splitter plate shows a more attenuated response with the splitter plate in. Results show there is between 12 to 20 percent steady-state coupling with splitter plate in against 39 to 57 percent steady-state coupling without splitter plate. Coupling is defined as the response of lower duct variables to disturbance introduced in upper duct only.

The results from the tests on the two-dimensional inlet were also compared to test results from a similar size 40-60 axisymmetric inlet. The response of the 70-30 two-dimensional inlet shows more attenuation in the 30- to 100-hertz region than the results from the 40-60 axisymmetric inlet.

An inherent instability in shock position was detected. This may be due to an excessively abrupt transition from square to circular cross-sectional area.

Using the experimental data, transfer functions were synthesized to describe the dynamic behavior. In general, the simplified transfer function was adequate in describing the inlet's dynamic response.

Lewis Research Center,
National Aeronautics and Space Administration,
Cleveland, Ohio, July 7, 1972,
764-74.

APPENDIX - SYMBOLS

A	bypass door area, cm^2
E	input signal to bypass doors, V
ESP	electronic shock position sensor
P	pressure, N/cm^2
Subscripts:	
a, . . . , h	refers to taps of the shock sensor
ℓ	refers to lower duct variables
u	refers to upper duct variables
57, 83	distance of pressure tap from cowl lip

REFERENCES

1. Wasserbauer, Joseph F.: Dynamic Response of a Mach 2.5 Axisymmetric Inlet with Engine or Cold Pipe and Utilizing 60 Percent Supersonic Internal Area Contraction. NASA TN D-5338, 1969.

2. Wasserbauer, Joseph F.; and Whipple, Daniel L.: Experimental Investigation of the Dynamic Response of a Supersonic Inlet to External and Internal Disturbances. NASA TM X-1648, 1968.

3. Wasserbauer, Joseph F.; and Willoh, Ross G.: Experimental and Analytical Investigation of the Dynamic Response of a Supersonic Mixed-Compression Inlet. Paper 68-651, AIAA, June 1968.

4. Neiner, George H.; Crosby, Michael J.; and Cole, Gary L.: Experimental and Analytical Investigation of Fast Normal Shock Position Controls for a Mach 2.5 Mixed-Compression Inlet. NASA TN D-6382, 1971.

5. Willoh, Ross G.: A Mathematical Analysis of Supersonic Inlet Dynamics. NASA TN D-4669, 1968.

6. Neiner, George H.: Servosystem Design of a High-Response Slotted-Plate Overboard Bypass Valve for a Supersonic Inlet. NASA TN D-6081, 1970.

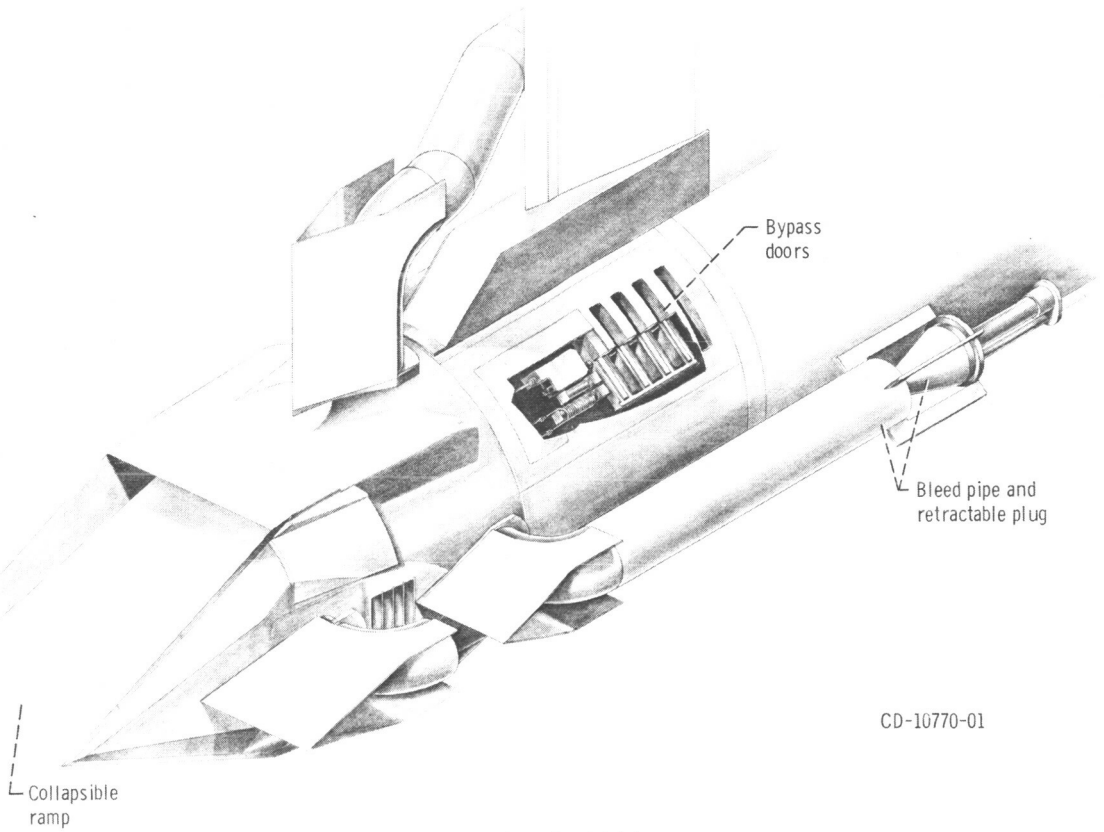

Figure 1. - Two-dimensional inlet.

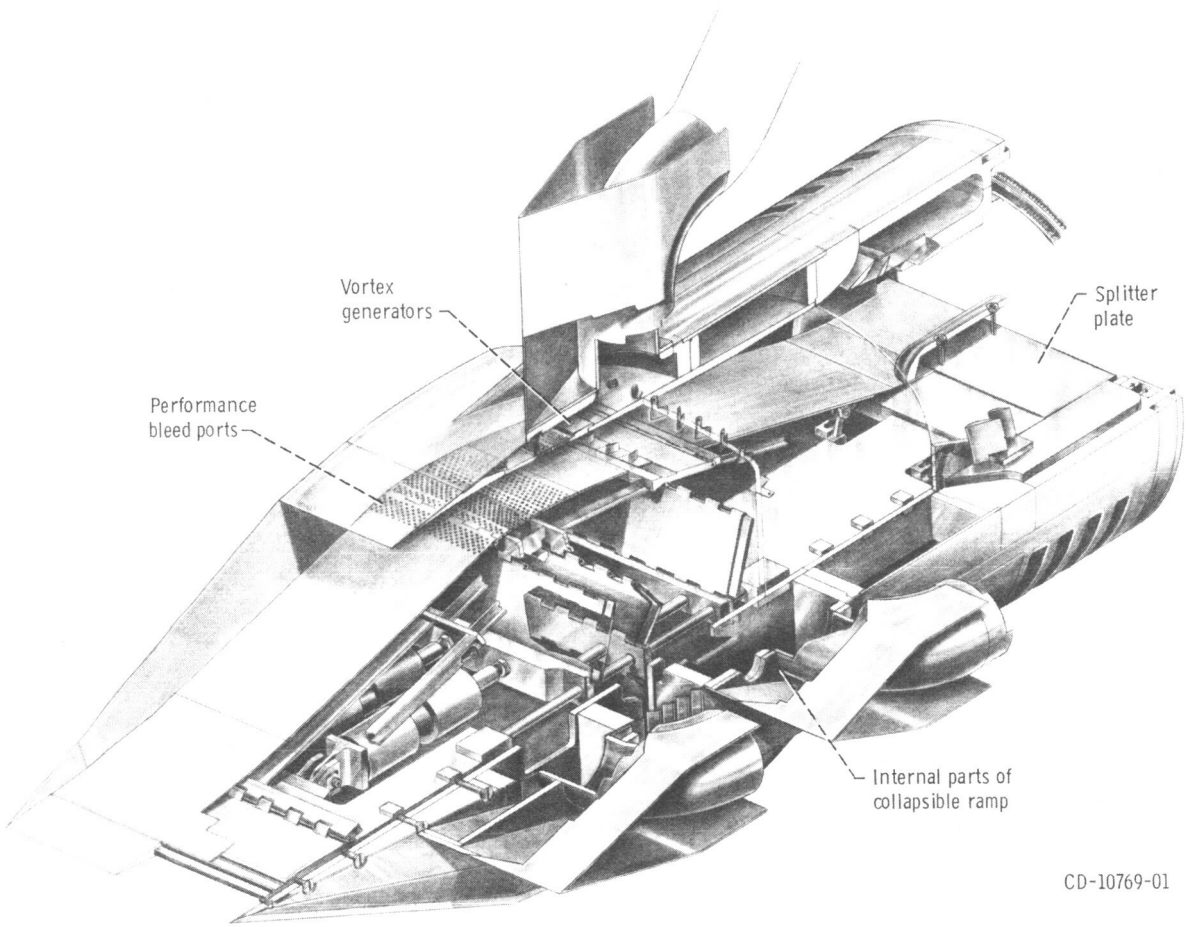

Figure 2. - Cutaway view of the two-dimensional inlet.

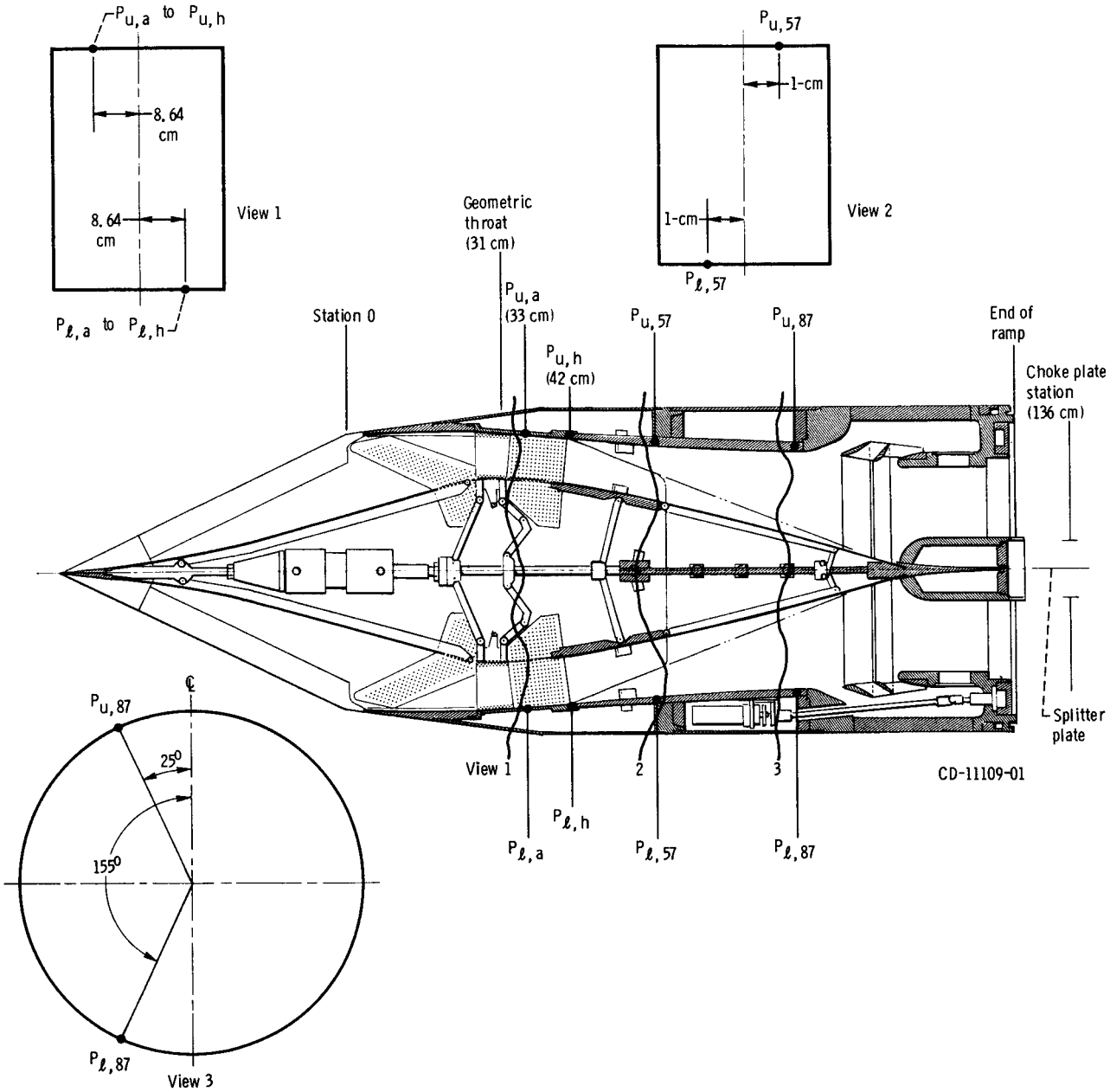

Figure 3. - Location of pressure transducers in upper and lower duct of two-dimensional inlet. Views 1, 2, and 3 show only inside cowl and/or sidewall surfaces, looking downstream.

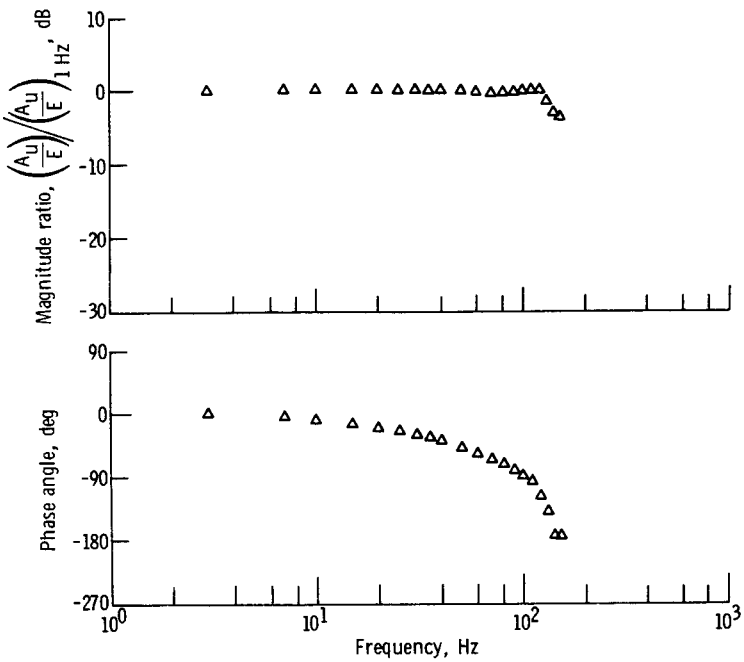

Figure 4. - Response of overboard bypass door to sinusoidal input voltage. Peak- to-peak movement of 0.42 centimeter (16 percent of maximum door travel).

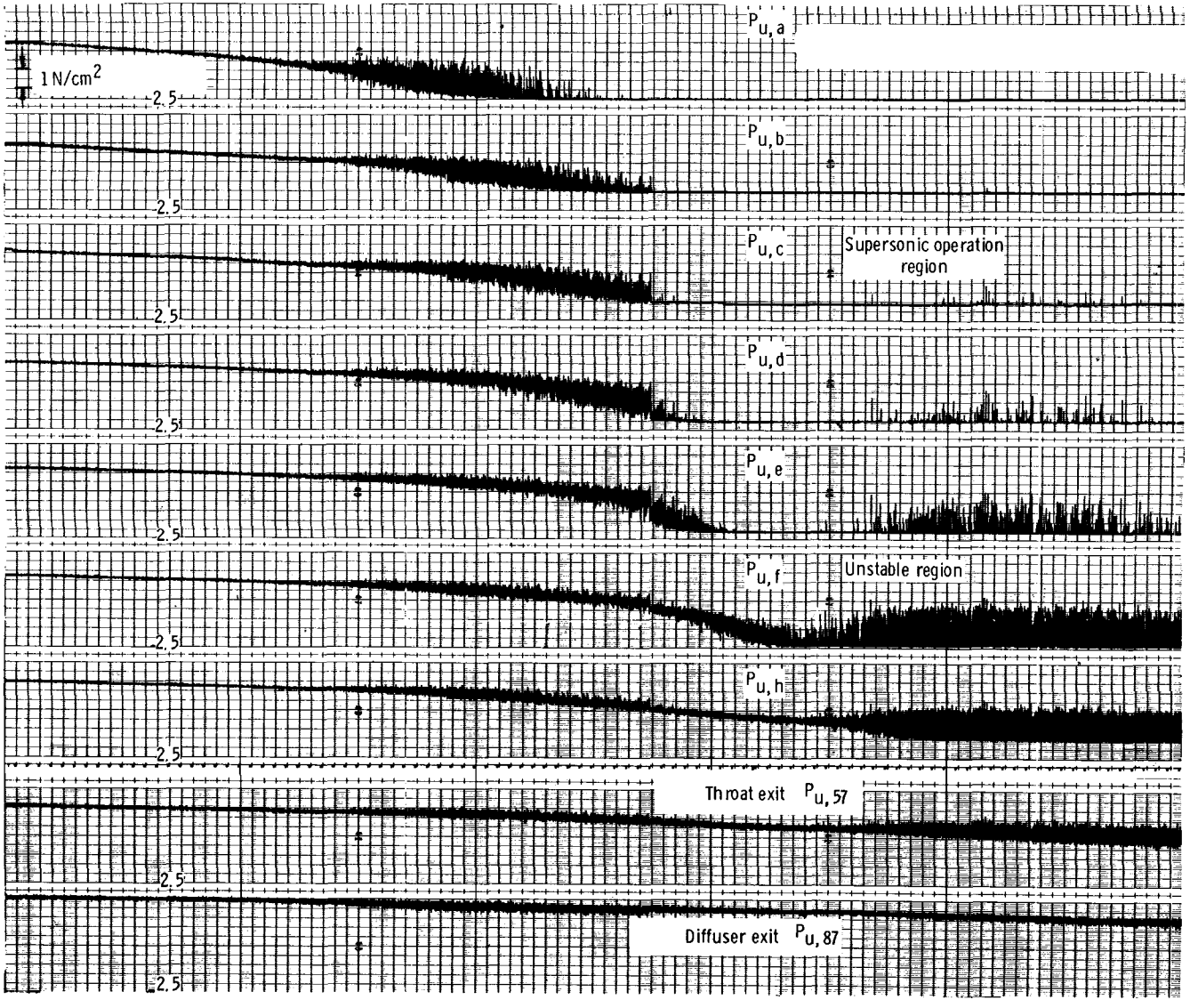

Figure 5. - Throat static pressure changes as terminal shock traverses inlet.

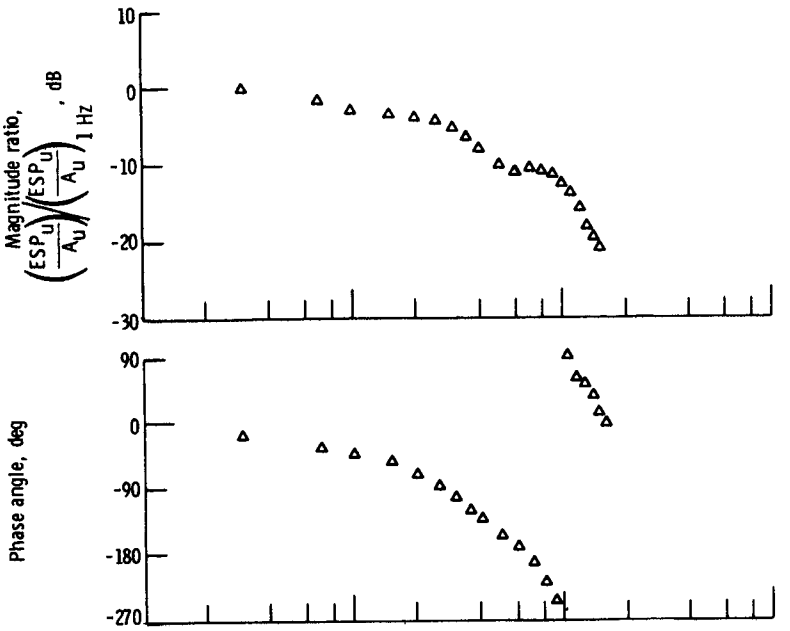

(a) Shock position ESP_u. Steady-state gain, 0.297 cm/cm^2.

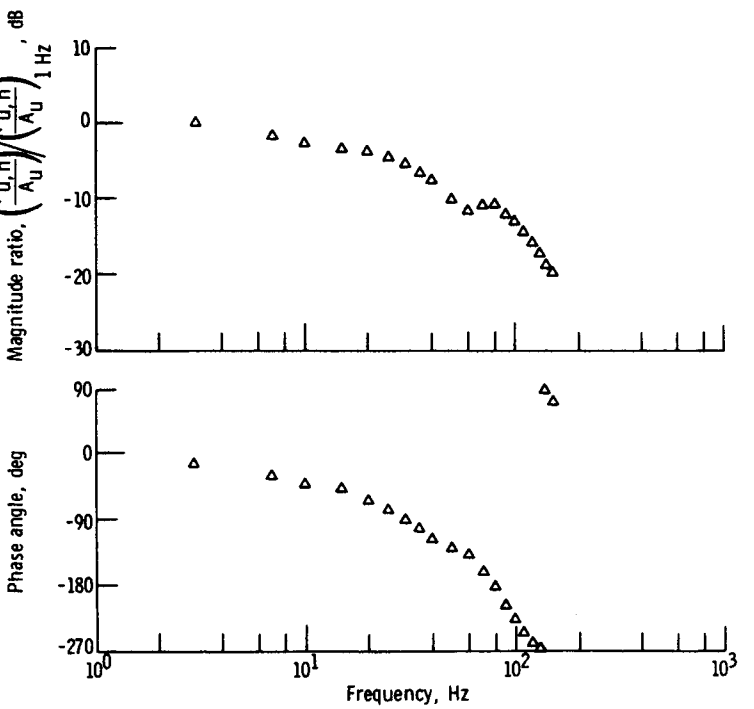

(b) Static pressure $P_{u,h}$. Steady-state gain, 0.048 $N/cm^2/cm^2$.

Figure 6. - Upper duct signals for upper duct bypass door oscillation. Zero angle-of-attack; backpressured bleeds; Mach 2.7.

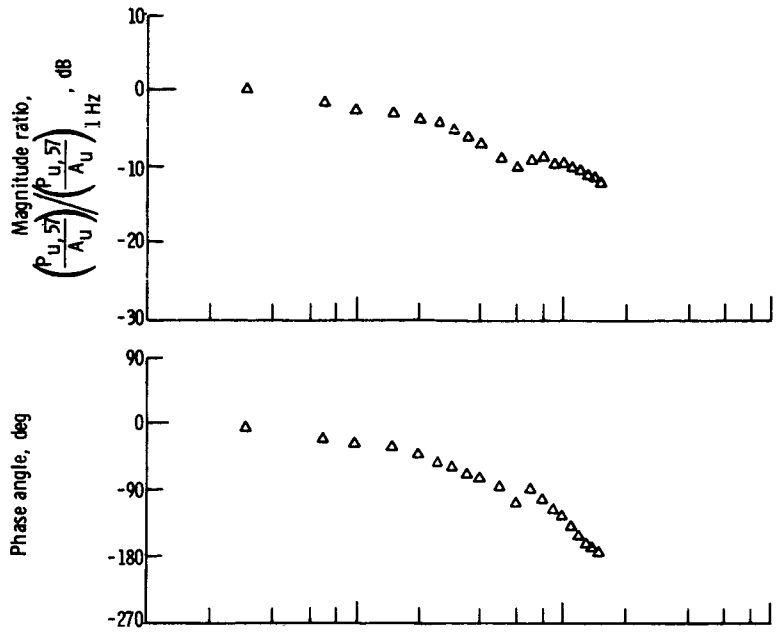

(c) Throat exit static pressure $P_{u,57}$. Steady-state gain, 0.026 $N/cm^2/cm^2$.

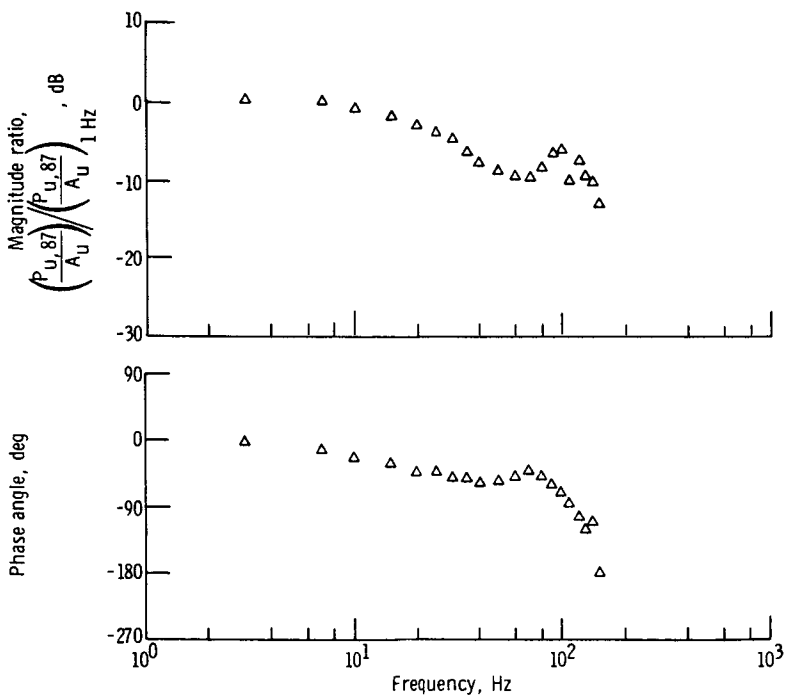

(d) Diffuser exit static pressure $P_{u,87}$. Steady-state gain, 0.016 $N/cm^2/cm^2$.

Figure 6. - Concluded.

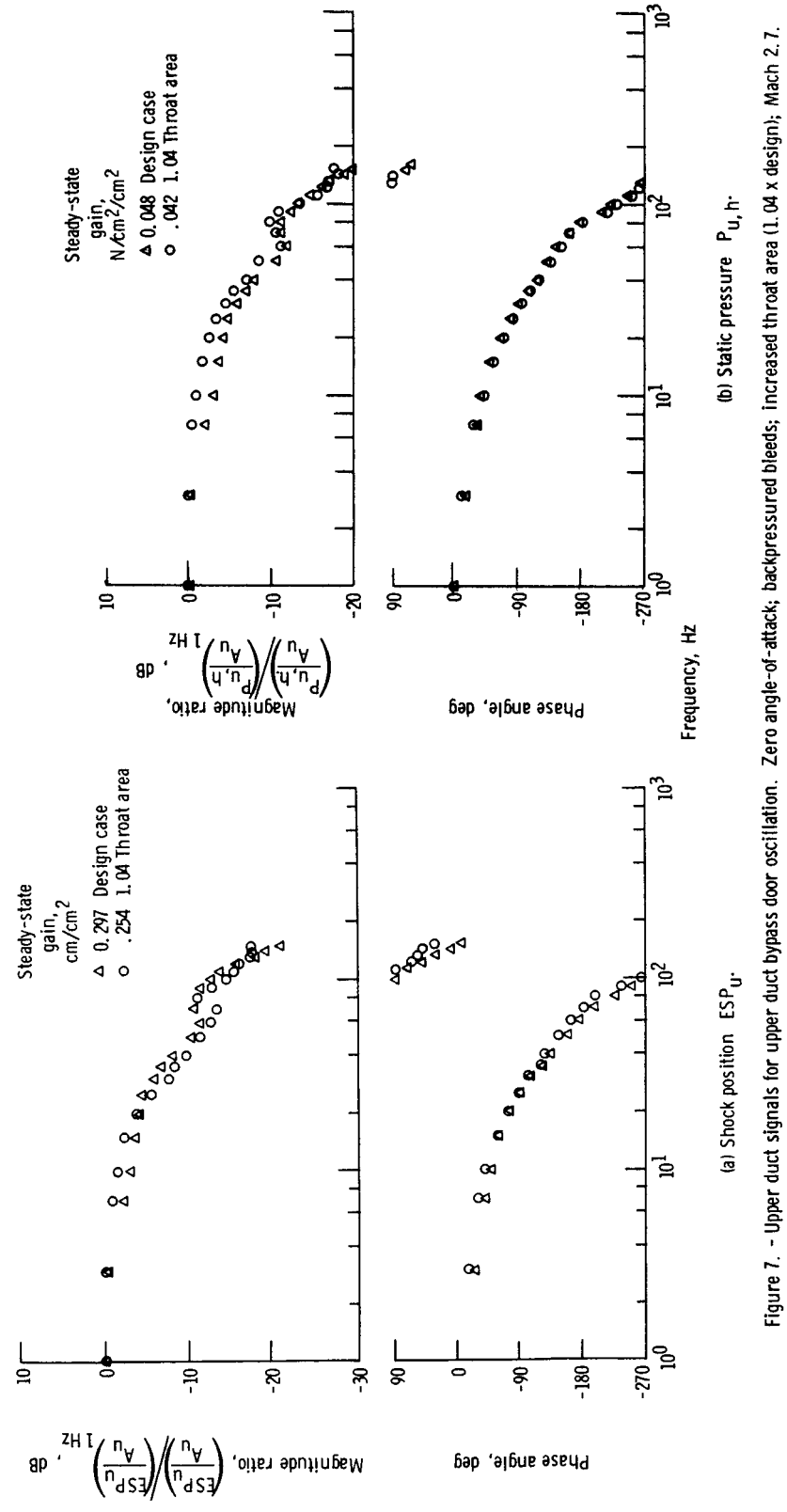

(a) Shock position ESP_U.

(b) Static pressure $P_{U,h}$.

Figure 7. - Upper duct signals for upper duct bypass door oscillation. Zero angle-of-attack; backpressured bleeds; increased throat area (1.04 x design); Mach 2.7.

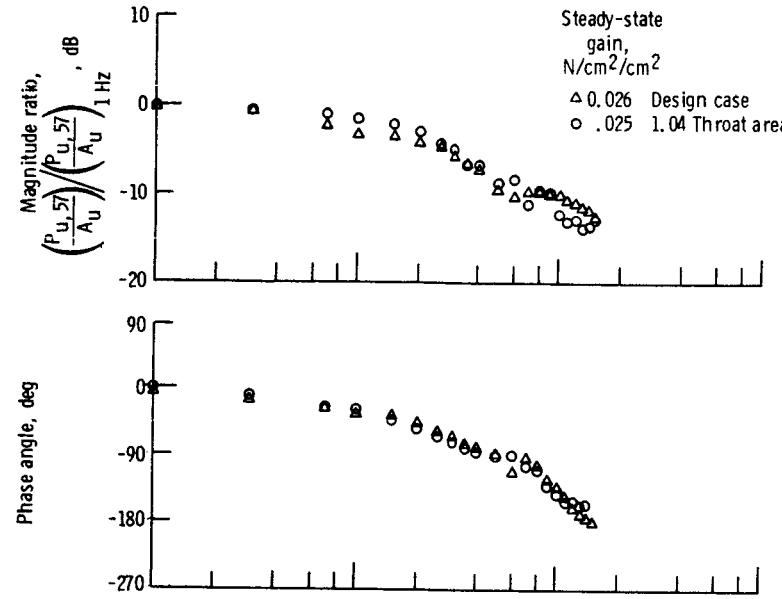

(c) Throat exit static pressure $P_{u,57}$.

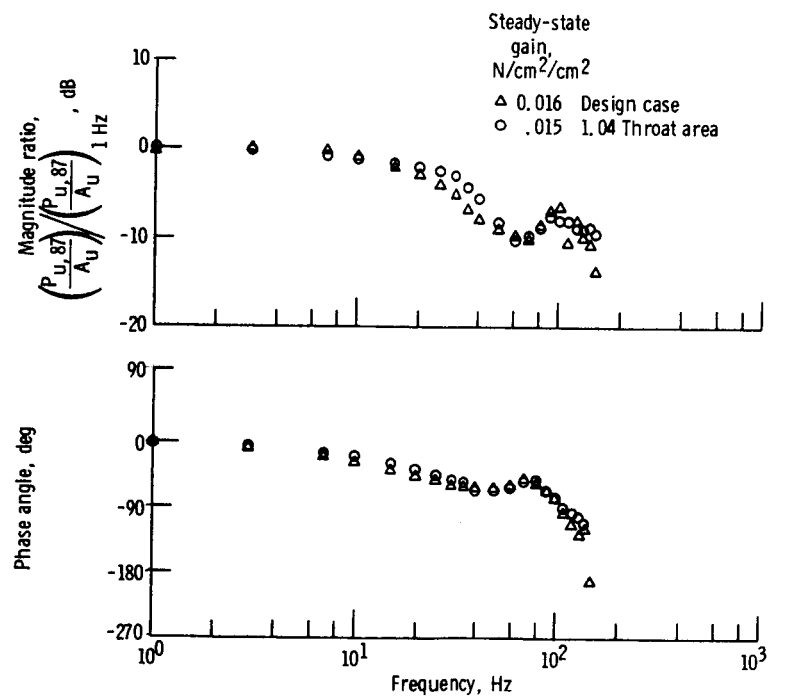

(d) Diffuser exit static pressure $P_{u,87}$.

Figure 7. - Concluded.

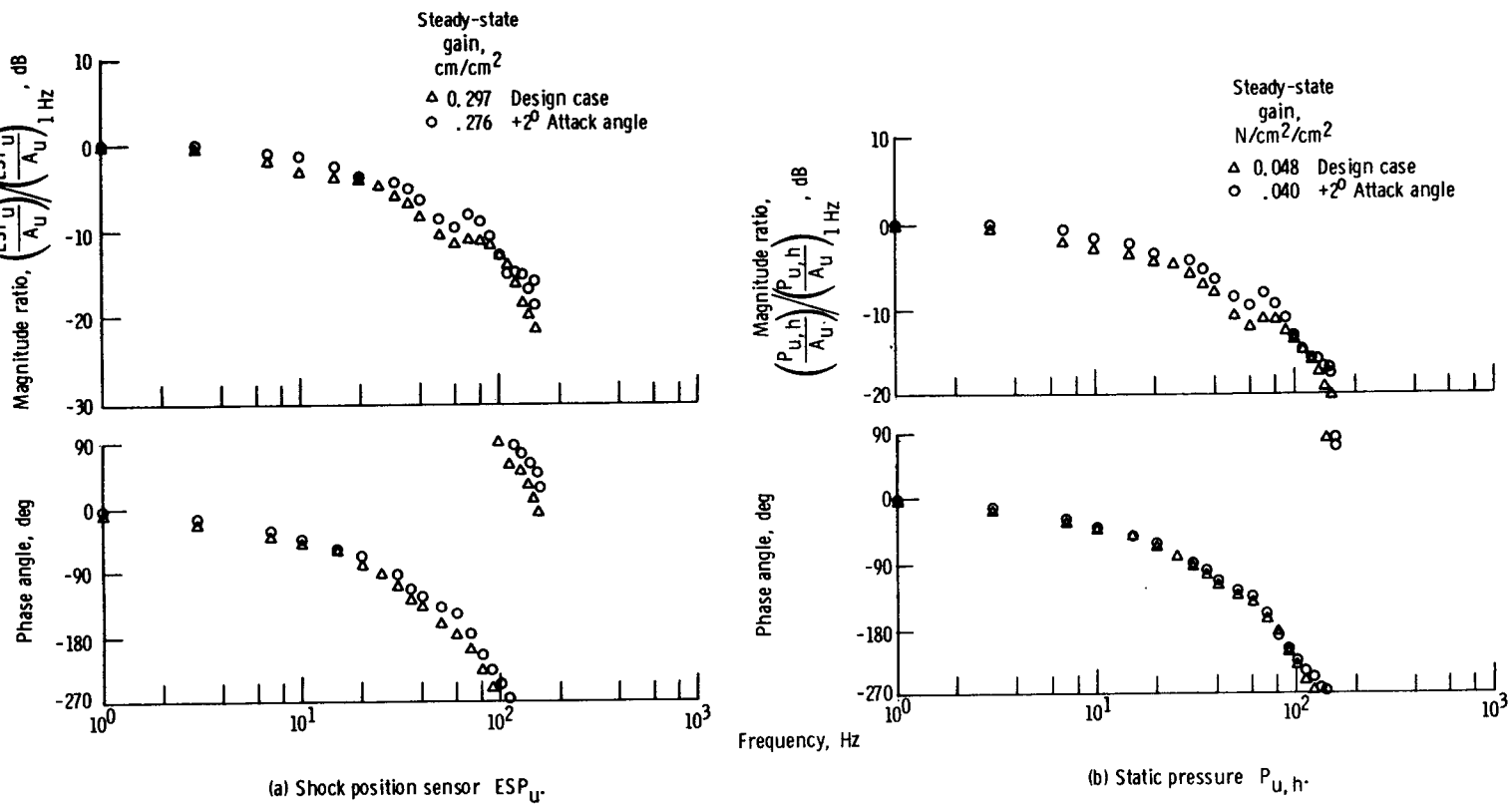

(a) Shock position sensor ESP_u.

(b) Static pressure $P_{u,h}$.

Figure 8. - Upper duct signals for upper duct bypass door oscillation. +2° Angle-of-attack; backpressured bleeds; Mach 2.7.

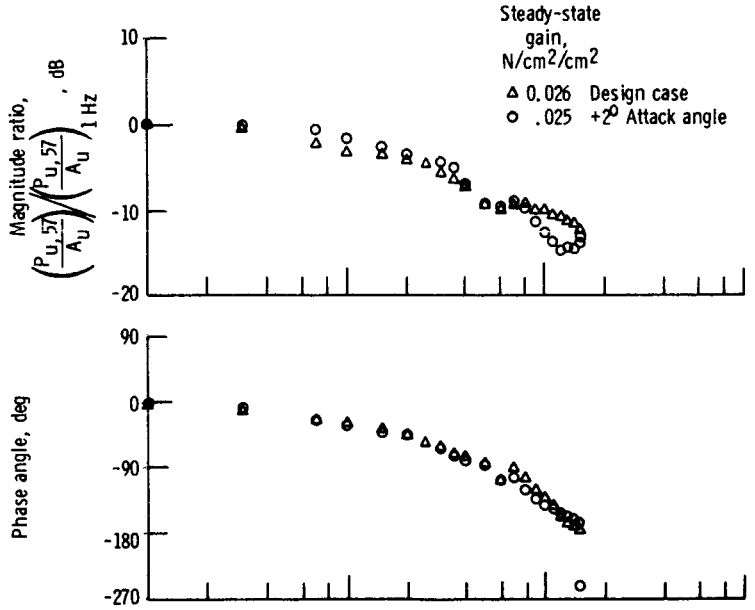

(c) Throat exit static pressure $P_{u,57}$.

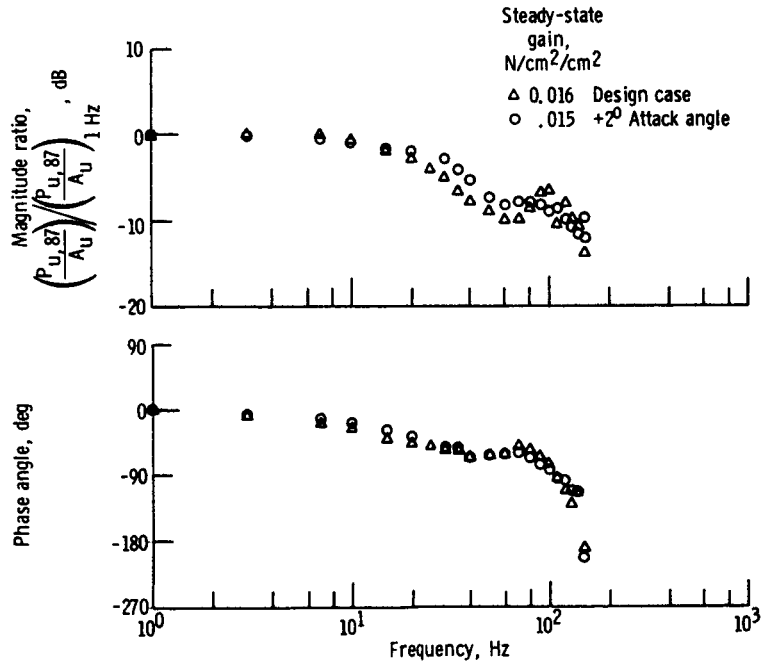

(d) Diffuser exit static pressure $P_{u,87}$.

Figure 8. - Concluded.

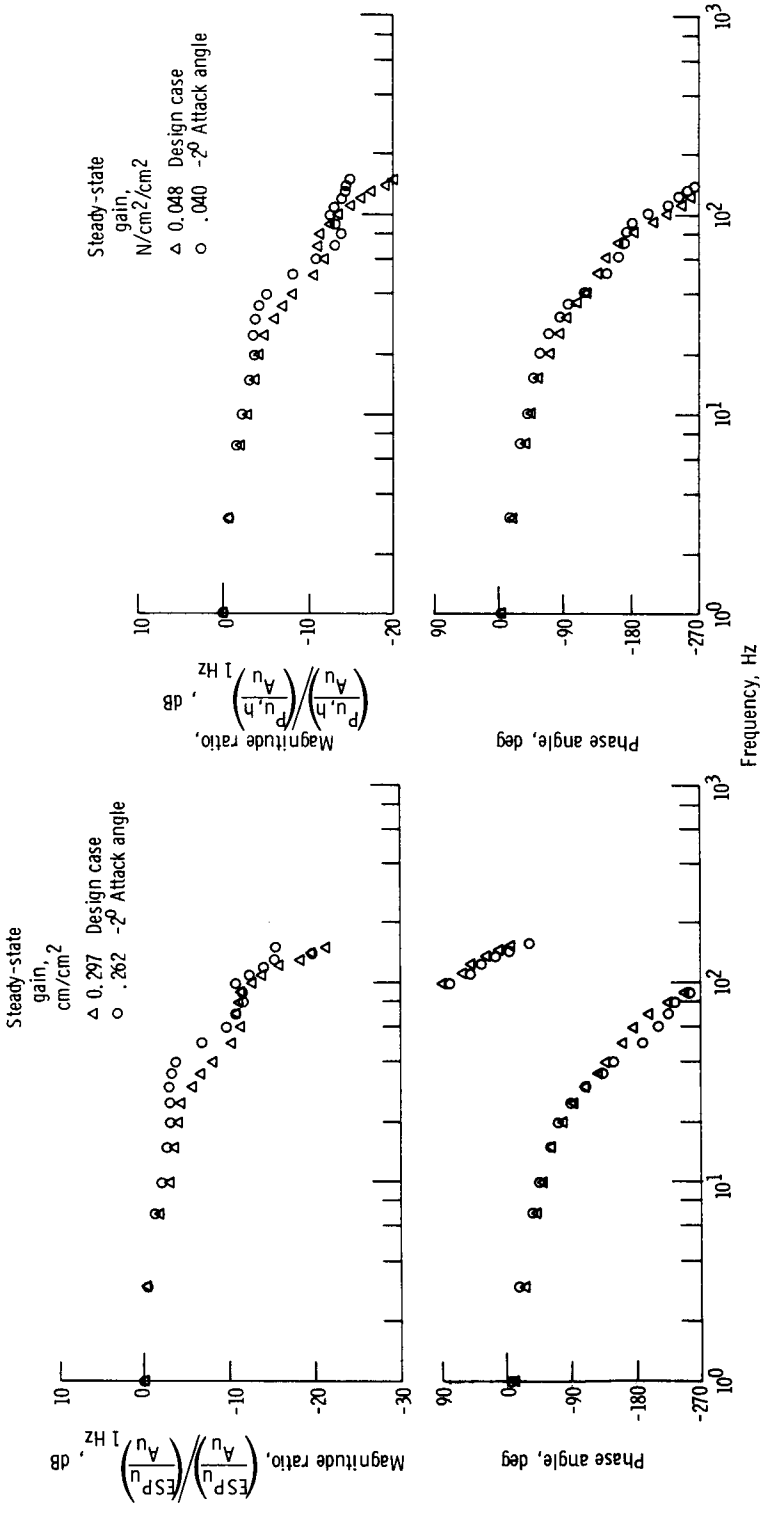

(a) Shock position ESP_U.

(b) Static pressure $P_{U,h}$.

Figure 9. - Upper duct signals for upper duct bypass door oscillation. -2° Angle-of-attack; backpressured bleeds; Mach 2.7.

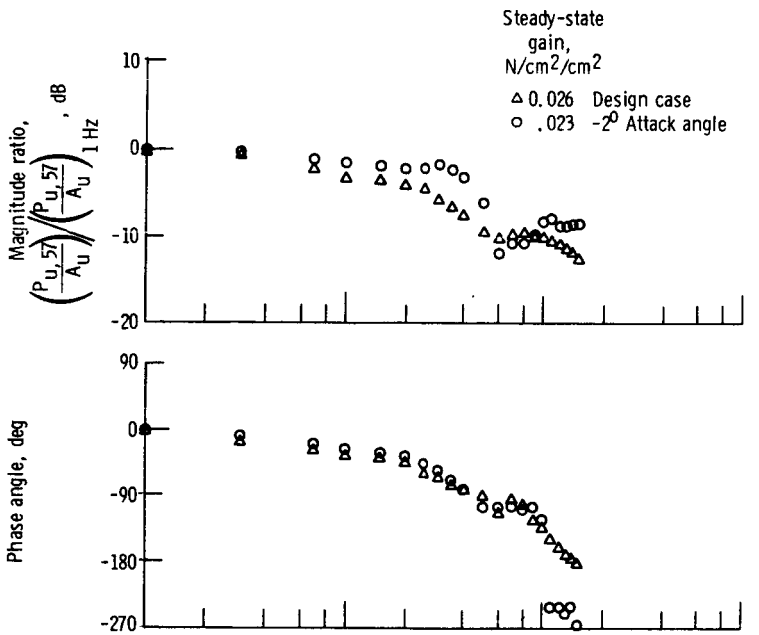

(c) Throat exit static pressure $P_{u,57}$.

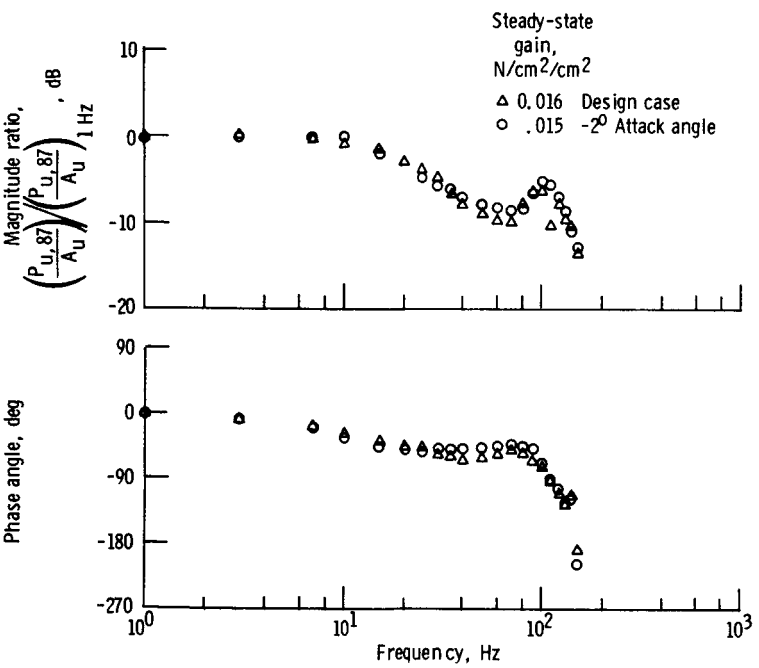

(d) Diffuser exit static pressure $P_{u,87}$.

Figure 9. - Concluded.

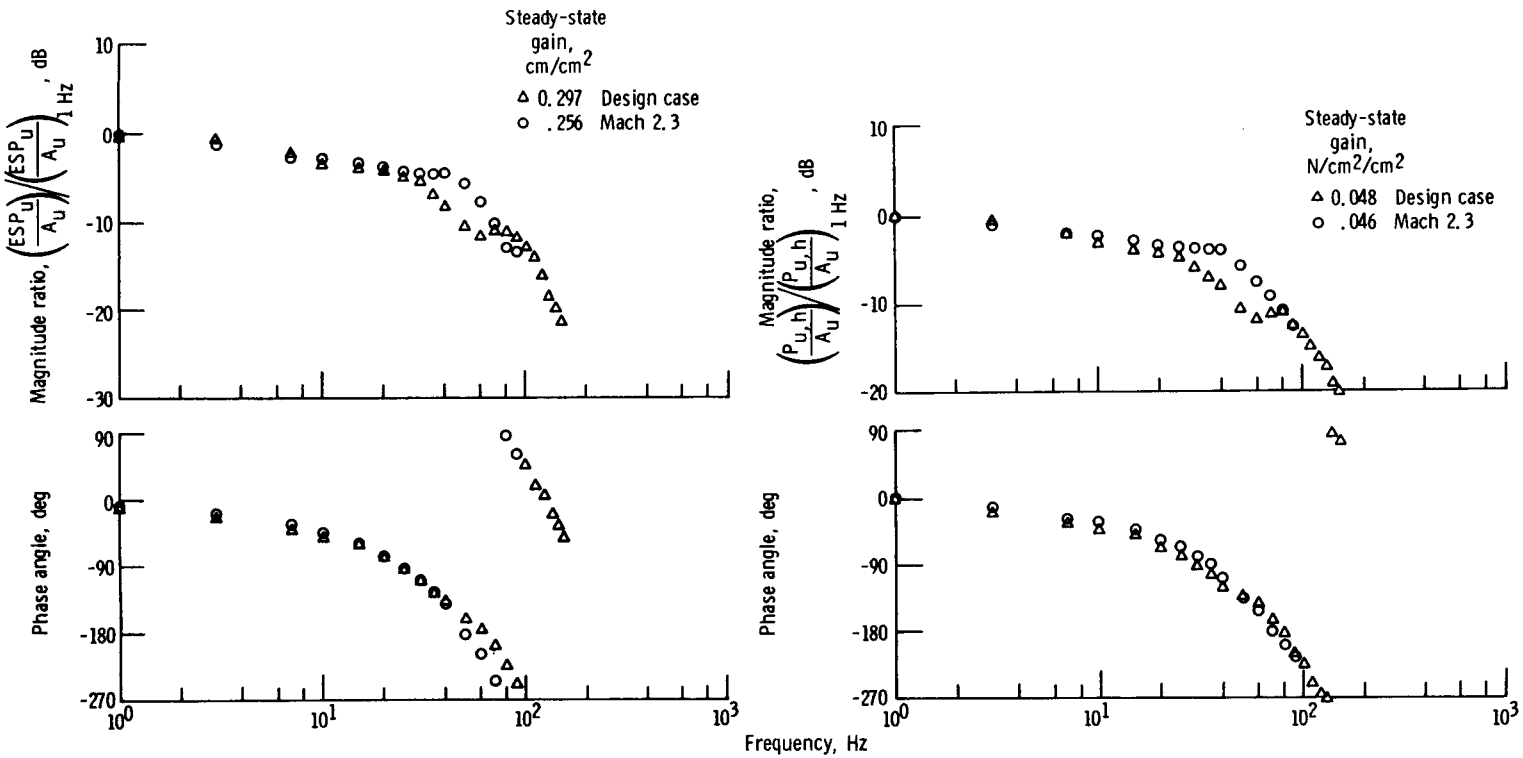

(a) Shock position ESP_u.

(b) Static pressure $P_{u,h}$.

Figure 10. - Upper duct signals for upper duct bypass door oscillation. Zero angle-of-attack; backpressured bleeds, Mach 2.3.

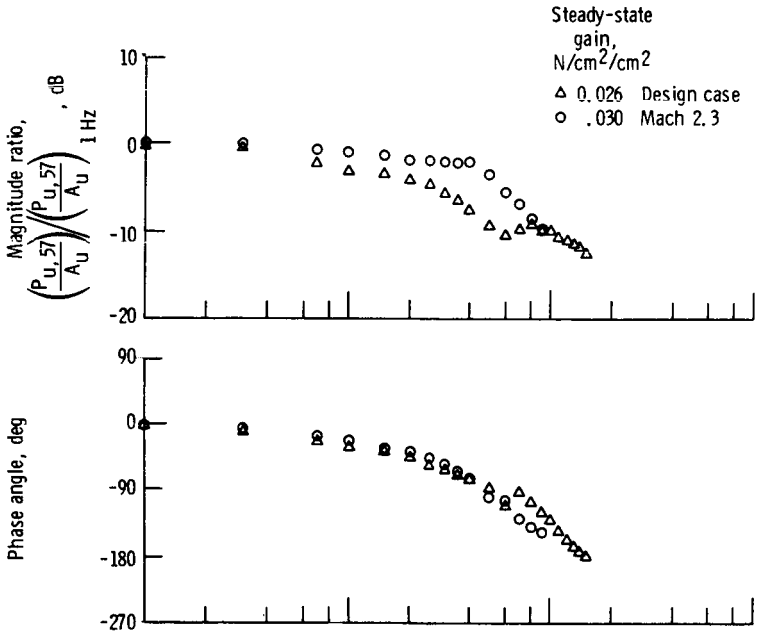

(c) Throat exit static pressure $P_{u,57}$.

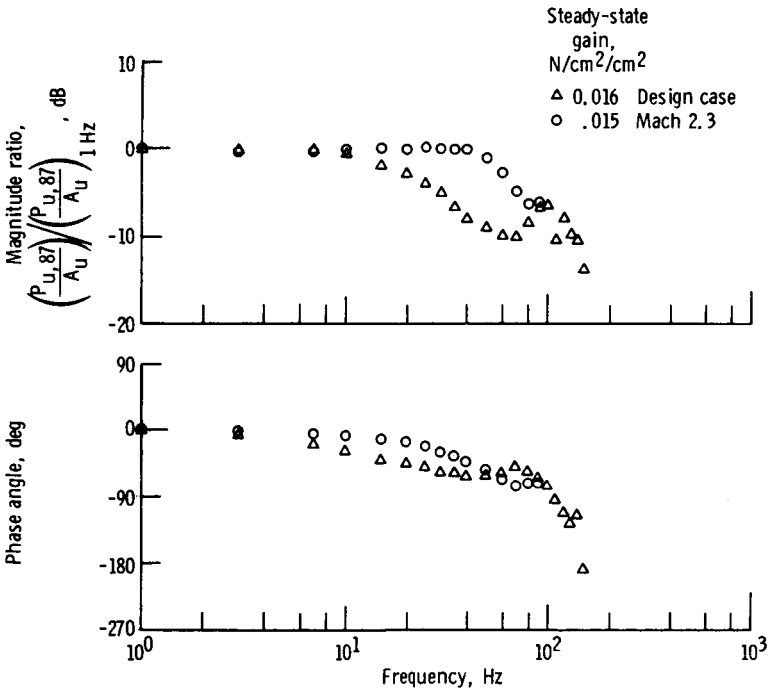

(d) Diffuser exit static pressure $P_{u,87}$.

Figure 10. - Concluded.

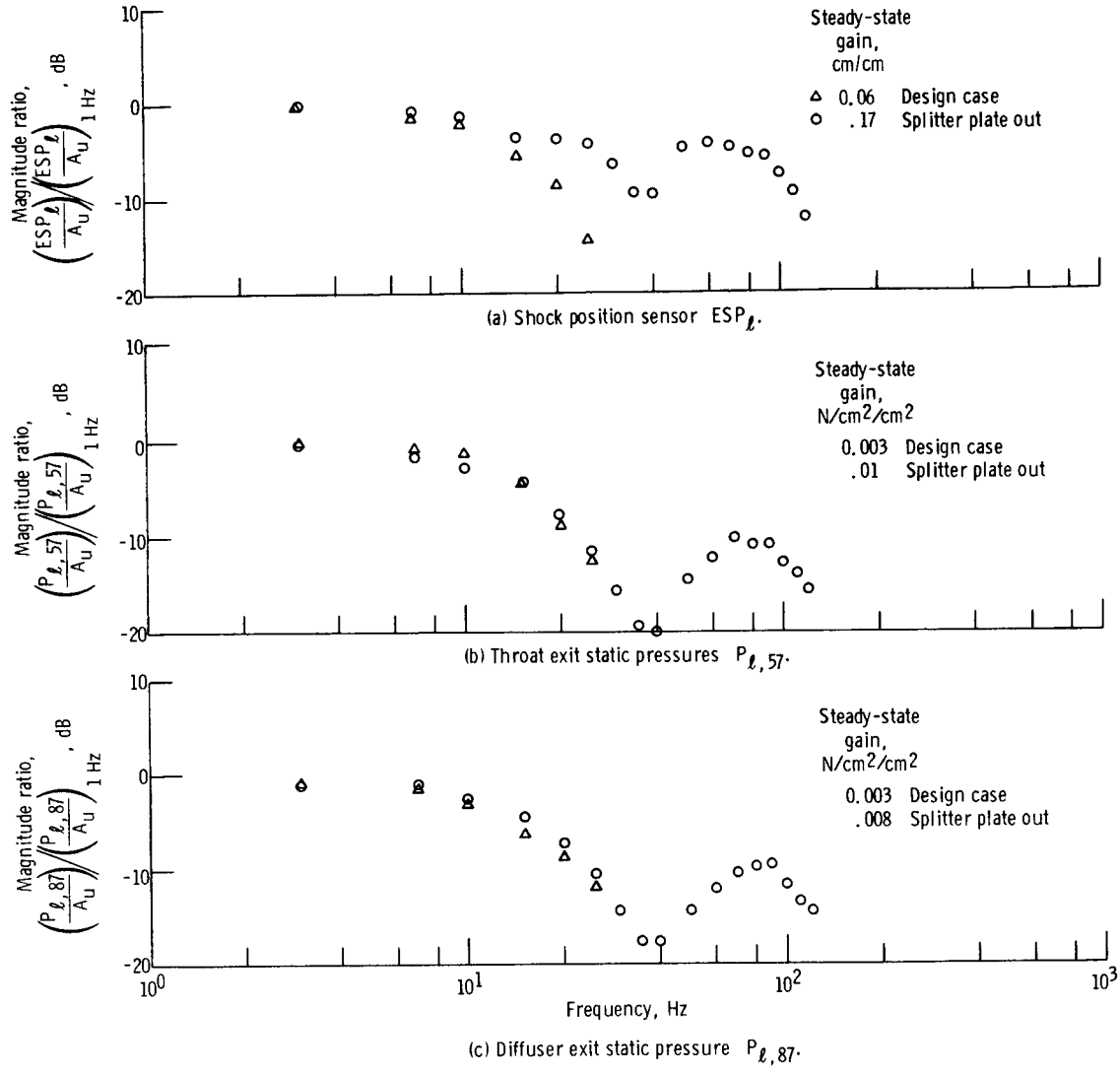

Figure 11. - Coupling between ducts (lower duct signals for disturbance in upper duct only) for inlet with and without splitter plate extension. Backpressured bleeds; Mach 2.7.

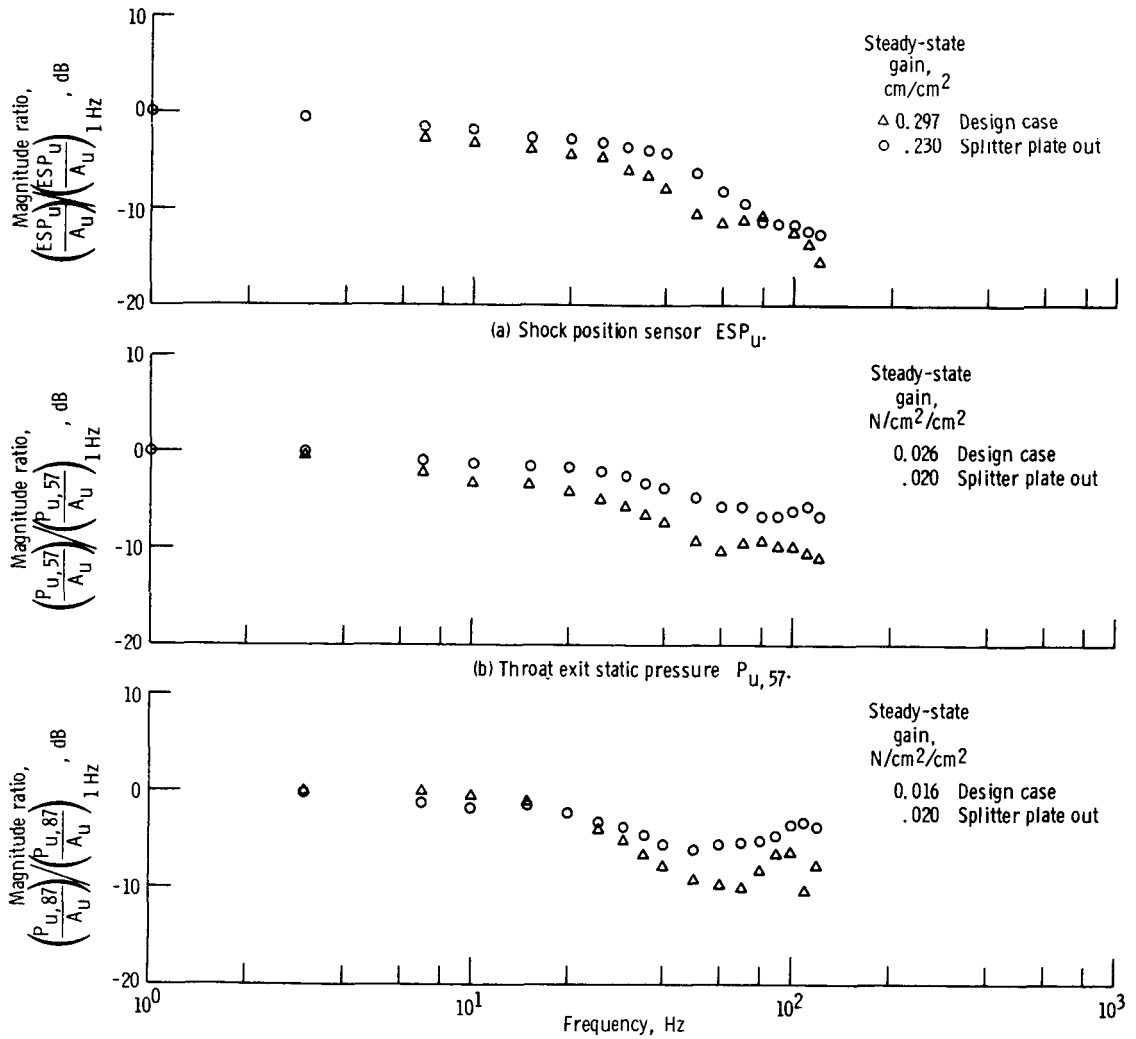

(a) Shock position sensor ESP_U.

(b) Throat exit static pressure $P_{U,57}$.

(c) Diffuser exit static pressure $P_{U,87}$.

Figure 12. - Upper duct signals for upper duct bypass door oscillation for inlet with and without splitter plate. Zero angle-of-attack; Mach 2.7.

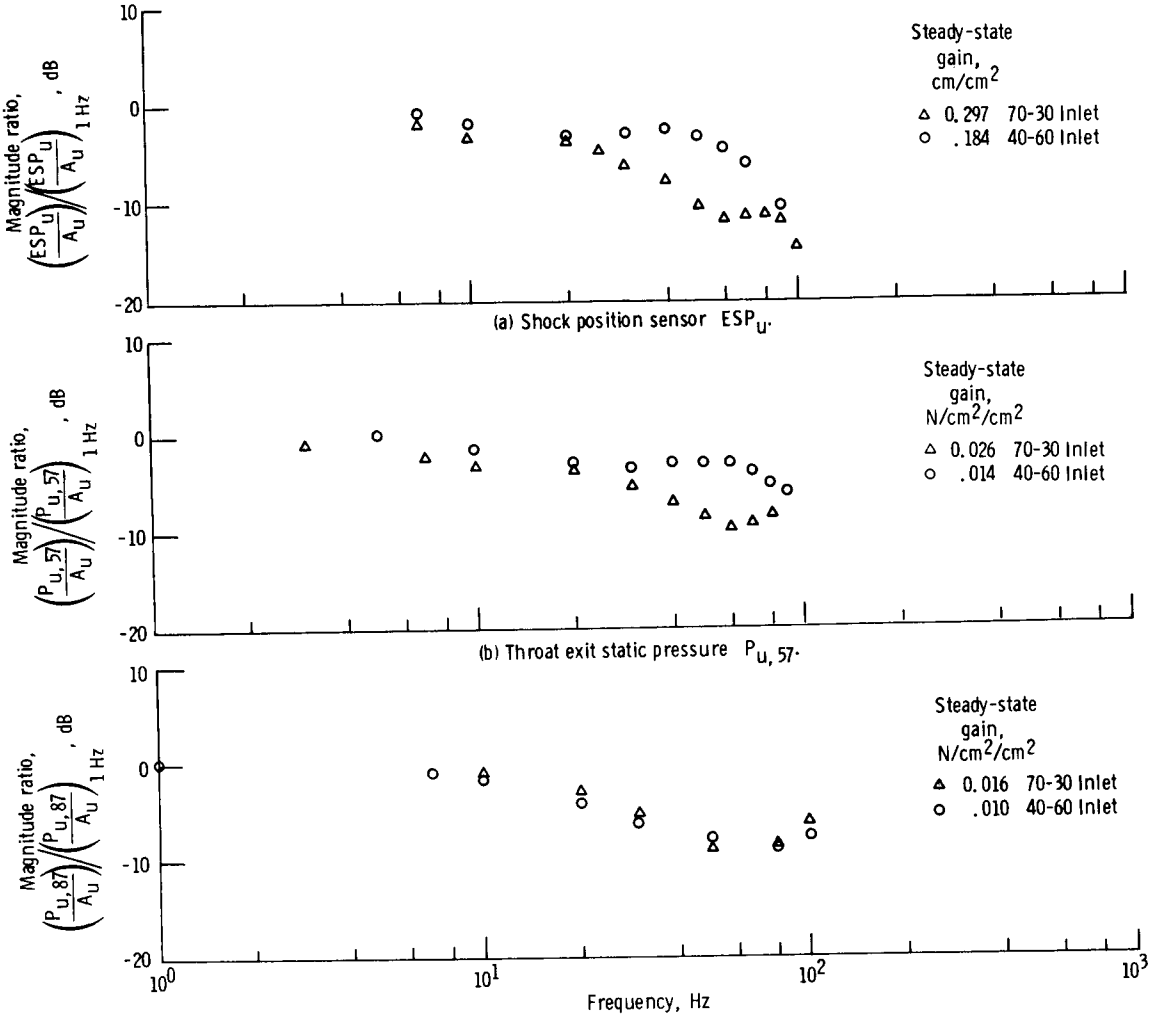

Figure 13. - Comparison of signals between 70-30 two-dimensional inlet and 40-60 axisymmetric inlet.

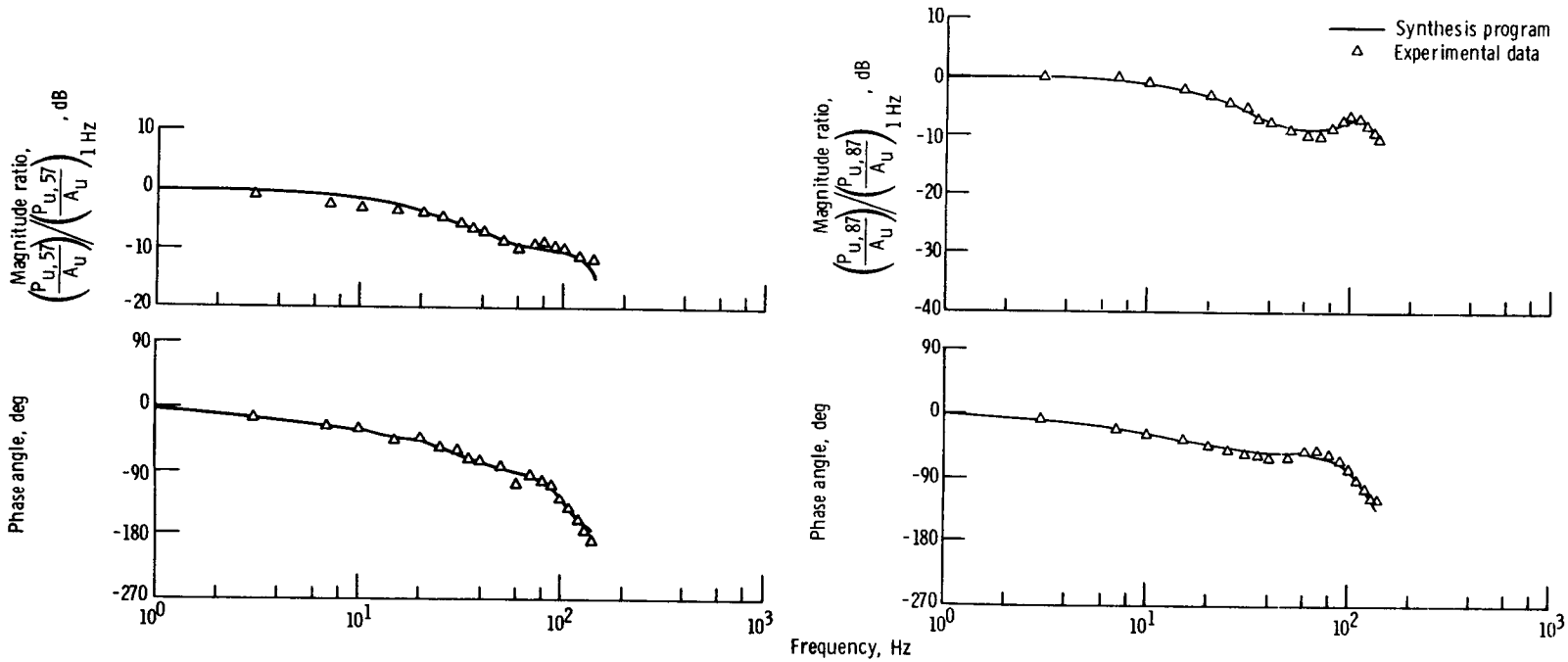

(a) Throat exit static pressure $P_{u,57}$. Synthesized transfer function:

$$\frac{\left(\frac{P_{u,57}}{A_u}\right)}{\left(\frac{P_{u,57}}{A_u}\right)_{1\,Hz}} = \frac{\left(1+\frac{S}{27}\right)}{\left[\frac{S^2}{(809)^2}+2\frac{(0.295)}{809}S+1\right]\left(1+\frac{S}{147}\right)\left(1+\frac{S}{22}\right)}$$

(b) Diffuser exit static pressure $P_{u,87}$. Synthesized transfer function:

$$\frac{\left(\frac{P_{u,87}}{A_u}\right)}{\left(\frac{P_{u,87}}{A_u}\right)_{1\,Hz}} = \frac{\left(\frac{S}{314}+1\right)\left(\frac{S}{312}+1\right)}{\left[\frac{S^2}{(785)^2}+2\frac{(0.282)}{785}S+1\right]\left(\frac{S}{142}+1\right)\left(\frac{S}{142}+1\right)}.$$

Figure 14. - Comparison of synthesized transfer function and experimental data.